

# Graphene nanosystems and low-dimensional Chern-Simons topological insulators

Y. H. Jeong and S. -R. Eric Yang \*

*Department of Physics, Korea University, Seoul, Korea*

A graphene nanoribbon is a good candidate for a  $(1+1)$  Chern-Simons topological insulator since it obeys particle-hole symmetry. We show that in a finite semiconducting armchair ribbon, which has two zigzag edges and two armchair edges, a  $(1+1)$  Chern-Simons topological insulator is indeed realized as the length of the armchair edges becomes large in comparison to that of the zigzag edges. But only a quasi-topological insulator is formed in a metallic armchair ribbon with a pseudogap. In such systems a zigzag edge acts like a domain wall, through which the polarization changes from 0 to  $e/2$ , forming a fractional charge of one-half. When the lengths of the zigzag edges and the armchair edges are comparable a rectangular graphene sheet (RGS) is realized, which also possess particle-hole symmetry. We show that it is a  $(0+1)$  Chern-Simons topological insulator. We find that the cyclic Berry phase of states of a RGS is quantized as  $\pi$  or  $0 \pmod{2\pi}$ , and that the Berry phases of the particle-hole conjugate states are equal each other. By applying the Atiyah-Singer index theorem to a rectangular ribbon and a RGS we find that the lower bound on the number of nearly zero energy end states is approximately proportional to the length of the zigzag edges. However, there is a correction to this index theorem due to the effects beyond the effective mass approximation.

PACS numbers:

## I. INTRODUCTION

Recently a rapid progress[1–4] has been made in the fabrication of graphene nanoribbons[5–10]. They have a great potential for spintronic applications, where electronic many-body interactions may play a significant role[7, 8, 10]. Nanoribbons may also provide numerous interesting issues in fundamental physics, such as topological insulators[11–18].

A nanoribbon is an excellent candidate for a Chern-Simons topological insulator since it obeys particle-hole symmetry, which is one of the symmetry requirements of low dimensional Chern-Simons topological insulators (this symmetry plays an important role in the  $Z_2$  classification of the Hamiltonians). A  $(1+1)$  dimensional Chern-Simons topological insulator is defined by a Lagrangian density[17] which involves the electric polarization  $\mathcal{P}$ [19–21]

$$\mathcal{L} = \mathcal{P} \epsilon^{\mu\nu} \partial_\mu A_\nu, \quad (1)$$

where  $A_\nu$  is the electromagnetic field. From the Lagrangian density follows that the current density is related to the polarization

$$j_\mu = -\epsilon_{\mu\nu} \frac{\partial \mathcal{P}}{\partial y_\nu}. \quad (2)$$

According to this Lagrangian one needs to show the presence of electric polarization to establish that a nanoribbon is indeed a Chern-Simons topological insulator. A

$(0+1)$  dimensional topological insulator can be also defined by a Chern-Simons effective Lagrangian[17]

$$\mathcal{L} = \text{Tr}[B_0], \quad (3)$$

where  $B_0$  is a Berry vector potential and the trace stands for the sum over the occupied states.

In the Chern-Simons theory one-dimensional Hamiltonians are labeled[17] by the parameter  $\theta$  such that for  $\theta = 0$  the Hamiltonian is  $Z_2$  trivial and for  $\theta = \pi$  the Hamiltonian is  $Z_2$  non-trivial. As the parameter  $\theta$  changes by  $2\pi$ , the polarization change,  $\Delta\mathcal{P} = \mathcal{P}(2\pi) - \mathcal{P}(0)$ , is given by the surface integral over a toroidal surface with the value equal to an integer in units of  $e$  (a first Chern number). Here the polarization of an occupied band is defined by the Zak phase  $Z$ , obtained from *dimensional reduction* by performing a one-dimensional cut of a two-dimensional Brillouin zone[22]

$$\mathcal{P}(\theta) = \frac{e}{2\pi} Z = \frac{e}{2\pi} \oint dk_y (-i) \langle \theta, k_y | \frac{\partial}{\partial k_y} | \theta, k_y \rangle, \quad (4)$$

where the  $|\theta, k_y\rangle$  are the periodic part of two-dimensional Bloch wavefunctions (from now on we will call this quantity the *reduced* Zak phase to contrast it to the one-dimensional Zak phase[21] defined in Eqs. (A2) and (A3)). When the integration over  $k_y$  in the reduced Zak phase is performed along a zigzag edge the Zak phase is zero while when integrated along an armchair edge it is  $\pi$ [22]. In contrast, it should be noted that, in translationally invariant one-dimensional systems the ordinary definition of the Zak phase is a multivalued quantity with a quantum uncertainty[15, 21, 23] (we will show this explicitly for graphene nanoribbons).

When translational invariance is broken the spatial variation of polarization can change abruptly and domain walls can be present in graphene nanoribbons: in

---

\*corresponding author, eyang812@gmail.com

a graphene zigzag ribbon translational invariance is broken along the *perpendicular* direction to the zigzag edges and the polarization changes suddenly across the zigzag edges. This effect is described by the Chern-Simons field theoretical result Eq.(2), where the coordinate  $y$  is along the perpendicular direction. The domain wall has nearly zero energy zigzag *edge* states, similar to quantum Hall systems. A periodic armchair ribbon is translationally invariant along the ribbon direction. This invariance can be broken by cutting the bonds transversely, which will produce two extra zigzag edges (see Fig.1). This will give rise to the spatial variation of polarization along the ribbon direction, and produce *end* states (domain walls) with nearly zero energy[12]. In such finite graphene armchair ribbons[5, 6, 8, 10] we find that a (1 + 1) Chern-Simons topological insulator is realized as the aspect ratio between the lengths of armchair and zigzag edges goes  $L_y/L_x \rightarrow \infty$ . We will show from the relation between charge and polarization, Eq.(2), that end states have a fractional charge, analogous to polyacetylene[14]: the polarization  $P(y)$  varies from 0 to  $e/2$  as a function of  $y$  along the ribbon direction. This is an important implication of the Lagrangian density, and is a hallmark of a non-trivial topological insulator. The corresponding charge density of an end state for metallic and semiconducting armchair ribbon decays exponentially with very different the decay lengths. In the metallic case with a pseudogap the decay length is comparable to the system size, and only a *quasi-topological* insulator is formed.

When the aspect ratio is  $L_y/L_x \sim 1$  under the condition  $L_x \lesssim 100\text{\AA}$  a RGS[24, 25] is formed. We show that it is a (0 + 1) Chern-Simons topological insulator with particle-hole symmetry intact. In this island-like system a Berry phase can be generated through modulation of the hopping parameter of a C-C bond. We find that some states of a RGS have a cyclic Berry phase of  $\pi \bmod 2\pi$  while other states have zero Berry phase. In addition, the Berry phases of particle-hole conjugate states are equal to each other  $\bmod 2\pi$ . We will show that it has also nearly zero energy edge states, which is another hallmark of topological insulators.

In both (1 + 1) and (0 + 1) Chern-Simons topological insulators we find, using the Atiyah-Singer index theorem[26], that number of nearly zero energy end states is proportional to the length of the zigzag edges. We find also a correction to this Atiyah-Singer result due to the effects beyond the effective mass approximation.

This paper is organized as follows. We compute the polarization near a domain wall in a finite graphene ribbon In Sec.II. In Sec.III, we compute a Berry phase of a RGS, and show that such a system is a (0 + 1) dimensional topological Chern-Simons insulator. The number of zero modes of a finite length zigzag edge is computed in Sec.IV, in addition to a correction to the Atiyah-Singer index theorem on the lower bound on the number of zero modes. Conclusions are given in Sec. V. In Appendix we show that the polarization a one-dimensional nanoribbon has a quantum uncertainty between the values 0 and  $\frac{e}{2}$

(modulo  $e$ ).

## II. ARMCHAIR RIBBON WITH BROKEN TRANSLATIONAL INVARIANCE: DOMAIN WALL AND FRACTIONAL CHARGE

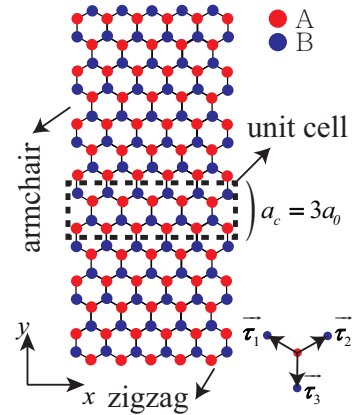


FIG. 1: Finite graphene ribbon has two zigzag edges and two armchair edges. When the length of the zigzag edges is  $L_x = 3La_0$  or  $(3L + 1)a_0$  a gap is present, but for  $L_x = (3L + 2)a_0$  no gap exists ( $L$  is an integer and  $a_0 = \sqrt{2}a$  is the unit cell length of the honeycomb lattice). Vectors  $\vec{\tau}_i$  connect a A carbon atom to three neighboring B carbon atoms. A unit cell of an armchair ribbon is shown in the dashed box.

Here we consider a spatial variation of the polarization and the formation of a fractional charge state. Cutting transversely the bonds of a periodic armchair ribbon breaks translational invariance and generates a *finite* length one-dimensional system with two zigzag edges at ends of the system, see Fig.1. Then outside of the armchair the system is trivial with  $\theta = 0$ , while inside the ribbon the system is non-trivial with  $\theta = \pi$ . In such an armchair ribbon, as the length of armchair edges becomes longer, doubly degenerate end states with nearly zero energy appear, as our tight-binding numerical results shown in Fig.2(a) demonstrate (the magnetic flux  $\phi$  is set to zero). Here the length of zigzag edges is  $L_x = 3La_0$  so that an energy gap[10] exist. In the limit where the length of the armchair edges  $L_y \rightarrow \infty$  we find that the decay length of the probability density of the end state is short, comparable to  $a_0$ , see Fig.2(b). This behavior is typical of a zigzag edge state[9]. These results are also true for a semiconducting armchair ribbon with different length of zigzag edges  $L_x = (3L + 1)a_0$ . In the metallic armchair ribbon with the length zigzag edges  $L_x = (3L + 2)a_0$  nearly zero energy end states also appear, see Fig.3(a). However, as shown in Fig.3(b) the decay length of these states are much longer, comparable to the system length. We will thus call this metallic armchair ribbon with a pseudogap a *quasi-topological insulator*.

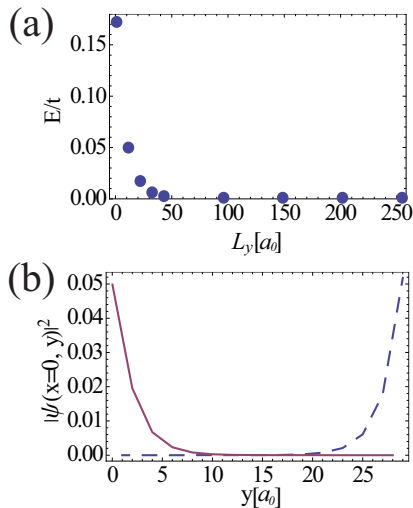


FIG. 2: Results for finite semiconducting armchair ribbon with a short width equal to the length of zigzag edges  $L_x = 3La_0 = 3a_0$ . (a) The eigenenergy of an end state vs the length armchair edges  $L_y$ . (b) Plot of the probability density,  $|\psi_M(x=0, y)|^2$ , of the state shown in (a) vs  $y$  for the length armchair edges  $L_y = 30a_0$ . The left zigzag edge ( $y = 0$ ) consists of *A*-carbons and the right edge ( $y = 3.52a_0$ ) of *B*-carbons. The red line indicates the value of the probability density on *A*-carbons and the blue line indicates the probability density on *B*-carbons.

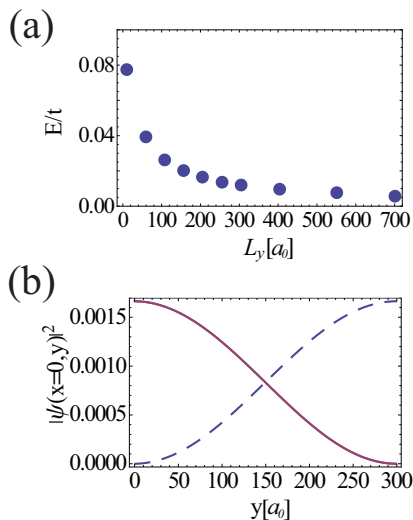


FIG. 3: Same as in Fig.2 but for the metallic case with the length zigzag edges  $L_x = (3L + 2)a_0 = 2a_0$ . From (b) we see that the width of domain wall is long, comparable to the length of the system  $L_y = 300a_0$ .

These probability densities satisfy the relation between polarization and charge of a Chern-Simons topological insulator, Eq.(2): for a semiconducting armchair ribbon (with a gap in the DOS) the *A*- or *B*-type probability density decays rapidly

$$\rho(y) = \frac{\partial \mathcal{P}(y)}{\partial y} \sim e^{-\alpha \frac{y}{a_c}}. \quad (5)$$

For a metallic armchair ribbon (with a pseudogap in the DOS) it decays slowly

$$\rho(y) = \frac{\partial \mathcal{P}(y)}{\partial y} \sim e^{-\beta \frac{y}{L_y}}, \quad (6)$$

where  $L_y$  is the length of the armchair edges. In the limit  $L_y \rightarrow \infty$  the integrated probability density on one type of carbon atoms gives the fractional charge, given by[17]

$$Q = \int_0^\infty dy \frac{\partial \mathcal{P}(y)}{\partial y} = P(\infty) - P(0) = -\frac{e}{2}. \quad (7)$$

The existence of this charge of one-half is thus related to the variation the polarization  $P(y)$  from 0 to  $-e/2$ . These end states with zero energy represent a fractional charge of  $1/2$ [12, 14, 18] of a domain wall (they appear in degenerate pairs[18, 27]).

### III. RECTANGULAR SHEET: (0 + 1) DIMENSIONAL CHERN-SIMONS TOPOLOGICAL INSULATOR

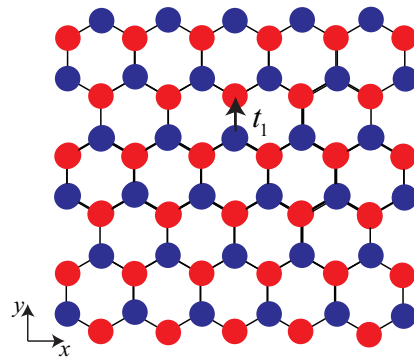


FIG. 4: RGS is shown. The length of armchair (zigzag) edges is  $L_y(L_x)$ . We choose a *C* atom and distort its hopping integral  $t_1$ . Adiabatic cycle is performed through the variation of  $t_1$ .

In the opposite regime  $L_y/L_x \sim 1$  with  $L_x \lesssim 100\text{\AA}$  a RGS is realized, see Fig.4. A RGS is an island-like system and is a (0 + 1) dimensional system. However, the effects

of armchair and zigzag edges may compete. It is thus unclear whether a RGS is a topological insulator. Here we investigate whether a RGS is really a Chern-Simons topological insulator. To establish that its effective Lagrangian is given by a  $(0+1)$  Chern-Simons topological field theory, Eq.(3), we need to construct non-vanishing Berry vector potentials.

It is not trivial to choose the appropriate adiabatic cyclic parameters. We use the following adiabatic cyclic parameters. We induce a time-dependent change of a C-C bond, see Fig.4. Its hopping parameter has time dependence  $t_1 = 0.9te^{i2\pi\tau/\tau_0}$  with  $0 \leq \tau/\tau_0 \leq 1$ . Note that this perturbation preserves particle-hole symmetry. The Berry vector potential of this  $(0+1)$  dimensional system is

$$B_0 = \sum_{\alpha} \langle \psi_{\alpha} | i \frac{d}{d\tau} | \psi_{\alpha} \rangle, \quad (8)$$

where the summation is over the occupied states. We use the tight-binding method in site-representation to compute the Berry phase since tight-binding approach is more accurate than the effective mass approach for small island-like systems. We use a gauge fixing to ensure numerically stable results[23].

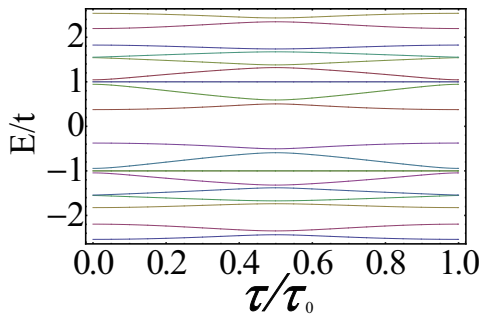


FIG. 5: Energy levels of a RGS vs  $\tau$ . The lengths are  $(L_x, L_y) = (3a_0, 3.52a_0)$ . Particle-hole symmetry is present.

To compute the Berry phase we first need to obtain eigenstates and eigenenergies as a function of the adiabatic parameter. The energy levels of a RGS are shown in Fig.5 as a functions of time  $\tau$ . Note that the computed energies display particle-hole symmetry. The computed Berry phases of the levels are either zero or  $\pi \bmod 2\pi$ [23], see Fig.6(a) ( $L_x = 3La_0$ ). Note the Berry phases of a pair of particle-hole conjugate states is equal each other mod  $2\pi$ . We have also found that the nearly zero energy zigzag edge states exist, see Fig.5. It has also nearly zero energy edge states, which is another hallmark of topological insulators,

When the length zigzag edges is  $L_x = (3L + 2)a_0$  the Berry phase is again either zero or  $\pi \bmod 2\pi$ , and the states in a particle-hole conjugate have the same value of Berry phase mod  $2\pi$ .

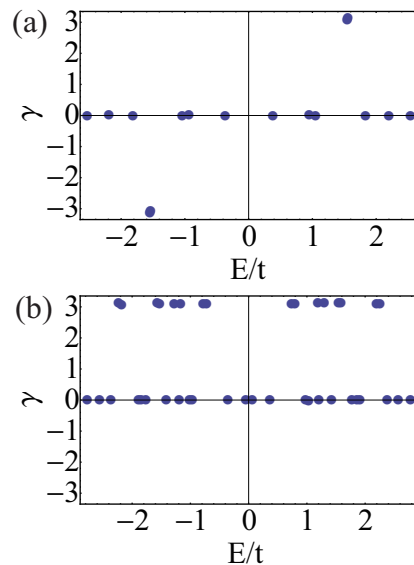


FIG. 6: Berry Phase of a RGS vs eigenenergies  $E$  when  $(L_x, L_y) = (3a_0, 3.52a_0)$  (a) and  $(L_x, L_y) = (5a_0, 3.52a_0)$  (b). In (a) we exclude points at  $E = \pm t$  because they are degenerated.

#### IV. NUMBER OF ZERO MODES

So far we have investigated nearly zero modes of narrow ribbons, i.e, zero modes of one-dimensional systems. We now study quasi-one-dimensional ribbons that have broader widths. We compute, as a function of the ribbon width, the number of nearly zero energy edge modes[22, 28] a finite length zigzag edge supports. The localization length of these edge modes increases with increasing energy. We choose to employ the Atiyah-Singer index theorem[26, 29] to compute the number of edge modes. We will show that it is proportional to the length of the zigzag edges. There is also a correction to this result, which we compute.

A RGS can be made out of an armchair ribbon by cutting C-C bonds along the transverse direction of the ribbon, which produces two zigzag edges. Mathematically this can be done by applying a chiral vector potential  $\vec{A}_c = (A_{c,x}\Theta(y), 0, 0)$  along the x-axis in a rectangle [18] (this area can be chosen as the unit cell shown in Fig.1). The bonds will be cut at the critical strength

$$\frac{eA_c v_F}{c} = t, \quad (9)$$

where  $\hbar v_F = \frac{3}{2}ta$  with the C-C distance  $a$ . Since the vector potential is chiral the relevant  $\mathbf{K}$  and  $\mathbf{K}'$  Dirac Hamiltonians are:

$$H_{\mathbf{K}} = v_F \vec{\sigma} \cdot (\vec{p} - \frac{e}{c} \vec{A}_c(\vec{r})) \quad (10)$$

for the  $\mathbf{K}$  valley, and

$$H_{\mathbf{K}'} = v_F \vec{\sigma}' \cdot (\vec{p} + \frac{e}{c} \vec{A}_c(\vec{r})) \quad (11)$$

for the  $\mathbf{K}'$  valley ( $e > 0$ ). The x and y components of  $\vec{\sigma}'$  are  $-\sigma_x$  and  $\sigma_y$ . Note that, unlike for the real vector potential, the chiral vector potential appears with opposite signs for  $\mathbf{K}$  and  $\mathbf{K}'$  valleys (it is chiral in the sense that it distinguishes valleys). In a RGS  $\mathbf{K}$  and  $\mathbf{K}'$  valleys are coupled by the armchair edges[30], and the effective mass Hamiltonian of a RGS is a block diagonal matrix with  $H_{\mathbf{K}}$  and  $H_{\mathbf{K}'}$  as blocks.

Since the Dirac operator is an elliptic operator, it is possible to employ the Atiyah-singer index theorem[29] (In the case of non-compact surfaces the theorem is applicable only when there is no net flux going through the open faces[31]). To apply the theorem we rewrite the  $\mathbf{K}$  valley Hamiltonian as

$$H_{\mathbf{K}} = \begin{pmatrix} 0 & P^\dagger \\ P & 0 \end{pmatrix}, \quad (12)$$

where the operator  $P^\dagger = \hbar v_F (\partial_x - i\partial_y - \frac{ie}{\hbar c} A_{c,x})$ . Then

$$H_{\mathbf{K}}^2 = \begin{pmatrix} P^\dagger P & 0 \\ 0 & P P^\dagger \end{pmatrix}. \quad (13)$$

We define  $\nu_+$  as the number of zero modes of  $P^\dagger P$  and  $\nu_-$  as the number of zero modes of  $P P^\dagger$ . Since there is no net flux the Atiyah-Singer index theorem dictates the difference in the numbers of zero modes is related to the vector potential

$$\text{index}(H_{\mathbf{K}}) = \frac{1}{2\pi\phi_0} \oint_C \vec{A}_c \cdot d\vec{l} = \nu_+ - \nu_- = 0, \quad (14)$$

where the contour C is along the edges of the rectangle. Non-zero contributions come from contour pieces  $C_1$  and  $C_2$ , where  $C_1 = -C_2$ . We have checked numerically that the numbers of zero modes from the contours  $C_1$  and  $C_2$  are identical, i.e.,  $\nu_+ = \nu_-$ . It should be noted that these zero modes also have *identical* wavefunctions. This implies that the index  $\nu_+$  is proportional to the line integral along  $C_1$ . The proportionality constant can be determined from the comparison with the tight-binding numerical result for the number of zero modes: we find that the total number of zero energy modes is proportional to the length of the zigzag edges  $L_x$

$$N_0 = \frac{1}{2\phi_0} \int_{C_1} \vec{A}_c \cdot d\vec{l} = \frac{A_c L_x}{2\phi_0} = \frac{1}{\sqrt{3}} \frac{L_x}{a_0}. \quad (15)$$

This number is equal to lower limit of the number of zero modes, see Fig.7. The tight-binding result shows that there is a correction to this result due to the effects beyond the effective mass approximation, see Fig.7.

There is another way to compute the number of nearly zero energy modes of a zigzag edge of length  $L_x$ . Consider a periodic zigzag ribbon with a finite length  $L_x$ , see Fig.8. For this system we can compute the exact number of zero modes using the tight-binding approach. In the tight-binding calculation[32, 33] the nearly zero eigenenergies

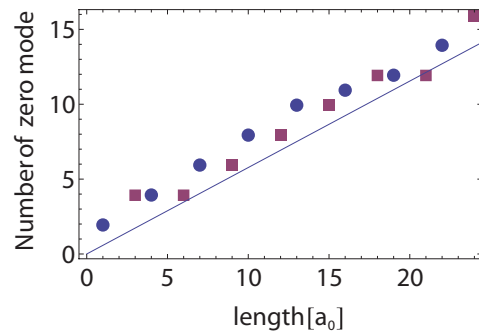


FIG. 7: Number of zero modes of a RGS, computed using the tight-binding Hamiltonian, are plotted as a function of the length of the zigzag edges  $L_x/a_0$ . Here the length of the armchair edges is  $L_y = 143.6a_0$ . Squares are for  $L_x = 3La_0$  and circles are for  $L_x = (3L+1)a_0$ . Note the number does not increase linearly with  $L_x$ . The lowest curve represents the lower bound and is given by the Atiyah-Singer result of Eq.(15).

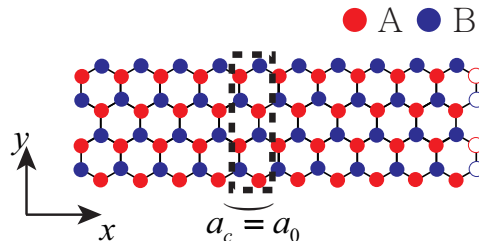


FIG. 8: A unit cell of a periodic zigzag ribbon is shown. The length of the unit cell is  $a_c = a_0$ .

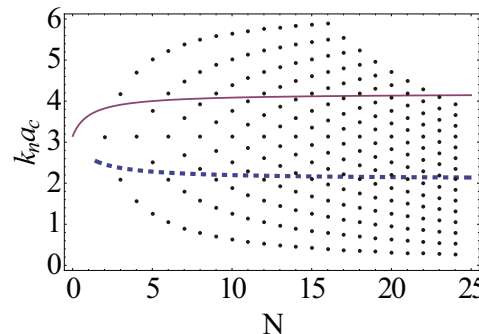


FIG. 9: For a periodic zigzag ribbon nearly zero modes exist at wavevectors  $k_n a_0 = 2\pi/N, 4\pi/N, \dots, 14\pi/N$ . These values are plotted as a function of  $N$ . Solid and dashed lines represent lower and upper bounds  $k_c^-(N)$  and  $k_c^+(N)$ .

are positive in the interval  $k_c^+(N) < k_n < \pi/a_0$  while they are negative in the interval  $\pi/a_0 < k_n < k_c^-(N)$ , where the values of the critical wavevectors are

$$k_c^\pm(N)a_0 = 2\cos^{-1} \left( \pm \frac{1/2}{1+1/N} \right) \quad (16)$$

with the periodic length  $L_x = Na_0$  ( $N$  is the number of unit cells and  $a_0$  is the unit cell length, see Fig.8). At the values  $k_c^+(N)$  and  $k_c^-(N)$  eigenenergies split from the bulk graphene energy spectrum. The number values of  $k_n$  satisfying these inequalities  $k_c^+(N) < k_n < k_c^-(N)$  are shown in Fig.9. We find that, as  $N$  increases, this number does not always increase monotonously, in contrast to the result of Atiyah-Singer, Eq.(15). Note that solutions at each  $k_n$  are nearly degenerate due to particle-hole symmetry, which gives an additional factor of 2. Thus, in total, the number of solutions must be multiplied by 2. This result for a zigzag ribbon is in agreement with the result of RGS for  $L_x \gg a_c$ : for  $N = 21$  we find 12 zero modes in both systems, see Figs.7 and 9. Also it should be noted that the numerical values of the number of zero modes are all even, consistent with the  $Z_2$  classification[27].

## V. SUMMARY

One of the symmetry requirements of low dimensional Chern-Simons topological insulators is particle-hole symmetry. Another important ingredient of the (1 + 1) Chern-Simons theory is a finite electric polarization defined by the Zak phase obtained from dimensional reduction. In a finite armchair ribbon with broken translational invariance a (1+1) Chern-Simons topological insulator is realized as the aspect ratio between the lengths of armchair and zigzag edges goes  $L_y/L_x \rightarrow \infty$ . However, only a quasi-topological insulator is formed in such a system when the energy gap goes to zero, i.e., in the metallic case with a pseudogap. In the opposite limit  $L_y/L_x \sim 1$  a (0 + 1) Chern-Simons topological insulator is realized, and the cyclic Berry phase is quantized as  $\pi$  or 0 (mod  $2\pi$ ). The Berry phases of particle-hole conjugate states are equal each other. In both armchair ribbon and RGS the number of nearly zero energy end modes is proportional to the length of the zigzag edges. A correction to this result that includes effects ignored in the effective mass approach is computed.

It will be interesting to measure the number of zero modes and the fractional charge in these systems. When a magnetic field is applied to a RGS time reversal symmetry is broken and more zero energy states will be formed[24, 34].

### Appendix A: Quantum uncertainty of polarization in nanoribbons

As we mentioned in Sec.I the one-dimensional Zak phase of periodic/infinite systems is a multivalued quantity with a quantum uncertainty (this is *not* the reduced Zak phase that enters in the Chern-Simons theory). When inversion/particle-hole symmetry is present in such a system polarization is quantized and can only take the value 0 or  $\frac{e}{2}$  (modulo  $e$ )[15, 17, 21, 23]. Although

the unit cell of a quasi-one-dimensional ribbon can contain numerous carbon atoms (see Fig.1) its polarization is expected to be quantized with the value 0 or  $\frac{e}{2}$  (modulo  $e$ ). Here we show this explicitly using a gauge invariant method.

We compute the one-dimensional Zak phase and polarization in the presence of a time-dependent vector potential  $A_y(\tau)$  along the direction of the ribbon (the period is  $T$ ). We choose the Coulomb gauge so that the electric field is  $E_y = -\frac{\partial A_y}{\partial \tau}$  (in the ribbon the electric field is applied along the  $y$ -axis). We relate the vector potential to the flux through

$$\phi = A_y(\tau)a_c, \quad (\text{A1})$$

where  $a_c$  is the unit cell length of the ribbon. The magnitude of the vector potential is chosen so that during the time interval  $T$  the flux  $\phi/\phi_0$  changes  $2\pi$  (in units  $\phi_0 = \frac{\hbar c}{e}$ ). The magnitude of the flux  $\phi$  will serve as an adiabatic parameter of a cyclic adiabatic evolution. Note that particle-hole symmetry of the band structure is *intact* as the flux changes.

The polarization is obtained by adding of the Zak phases of the occupied subbands  $l$

$$\mathcal{P} = -e \sum_{l=1}^{l'} \int_{-\pi/a_c}^{\pi/a_c} \frac{dk}{2\pi} A_k^l, \quad (\text{A2})$$

where  $k$  is the wavevector along the ribbon direction (the vector potential appears with it, i.e.,  $k + A_y$ ). Note that the subband index  $l$  is discrete while in Eq.(4) the corresponding variable  $\theta$  is continuous. Here the Berry vector potential is

$$A_k^l = i \langle u_{lk} | \frac{\partial}{\partial \phi} | u_{lk} \rangle, \quad (\text{A3})$$

where the periodic function  $u_{lk}(r)$  is defined by the Bloch wavefunction  $\psi_{lk}(r) = e^{ikr} u_{lk}(r)$ . When there are band crossings, i.e., degeneracy points, the Berry phase must be computed carefully.

One can compute numerically the polarization  $\mathcal{P}$  using the following *gauge-invariant* method[19, 20]

$$\mathcal{P} = \frac{e}{2\pi} \sum_{s=0}^{N_s-1} \frac{1}{N_s} \text{Arg} [\det \langle \tilde{u}_{lk_s} | \tilde{u}_{l'k_{s+1}} \rangle]. \quad (\text{A4})$$

The periodic function  $\tilde{u}_{lk}(r)$  is defined by  $u_{lk}(r) = \frac{1}{\sqrt{N_s}} \tilde{u}_{lk}(r)$ . Note that the normalization of  $\tilde{u}_{lk}(r)$  is such that  $\langle \tilde{u}_{lk} | \tilde{u}_{lk} \rangle = \int_{cell} dr \tilde{u}_{lq}^*(r) \tilde{u}_{lq}(r) = 1$ . Here we have discretized the Brillouin zone into small  $N_s$  intervals and the discrete wavevectors are  $q_s$  with the index  $s = 0, \dots, N_s - 1$  so that  $k_0 = -\pi/a_c$  and  $k_{N_s} = \pi/a_c$ . The overlap  $\langle \tilde{u}_{lk_s} | \tilde{u}_{l'k_{s+1}} \rangle$  is between valence subband wavefunctions at the adjacent wavevectors. It is computed

using the wavefunctions obtained from a tight-binding Hamiltonian. The angle  $\text{Arg} [\det \langle \hat{u}_{lq_s} | \hat{u}_{l'q_{s+1}} \rangle]$  can be chosen from the interval  $[0, 2\pi]$  or  $[-\pi, \pi]$ [35]. In the first case the computed value of the Zak phase is  $\pi$  while in the second case it is 0. We have verified this for both

periodic armchair and zigzag ribbons. In the presence of inversion symmetry this uncertainty related to two possible positions of the center of the Wannier functions[21]. This result holds both for armchair and zigzag ribbons.

- 
- [1] K. S. Novoselov, A. K. Geim, S. V. Morozov, D. Jiang, M. I. Katsnelson, I.V. Grigorieva, S. V. Dubonos and A. A. Firsov, Nature **438**, 197 (2005)
- [2] Y. Zhang, Y. -W. Tan, H. L. Stormer and P. Kim, Nature **438**, 201 (2005).
- [3] J. Cai, P. Ruffieux, R. Jaafar, M. Bieri, T. Braun, S. Blankenburg, M. Muoth, A. P. Seitsonen, M. Saleh, X. Feng, K. Mullen, and R. Fasel, Nature **466**, 470 (2010).
- [4] T. Kato and R. Hatakeyama, Nature Nanotech. **7**, 651 (2012).
- [5] M. Fujita, K. Wakabayashi, K. Nakada, K. Kusakabe, J. Phys. Soc. Jpn., **65**, 1920 (1996).
- [6] L. Brey and H. A. Fertig, Phys. Rev. B **73**, 235411 (2006).
- [7] Y. W. Son, M. L. Cohen, and S. G. Louie, Nature **444**, 347 (2006).
- [8] L. Yang, C.-H. Park, Y.-W. Son, M. L. Cohen, and S. G. Louie, Phys. Rev. Lett. **99**, 186801 (2007).
- [9] A. H. Castro Neto, F. Guinea, N. M. R. Peres, K. S. Novoselov, and A. K. Geim, Rev. Mod. Phys. **81**, 109 (2009).
- [10] J. W. Lee, S. C. Kim, and S. -R. Eric Yang, Solid State Commun. **152** (2012).
- [11] B.A. Bernevig and T. L. Hughes, *Topological insulators and topological superconductors* (Princeton University, 2013).
- [12] A. Y. Kitaev, Usp. Fiz. Nauk **171**, 131 (2001).
- [13] M.Z.Hansan and C.L. Kane, Rev. Mod. Phys. **82**, 3045 (2010).
- [14] A. J. Heeger, S. Kivelson, and J. R. Schrieffer, W. -P. Su, Rev. Mod. Phys., **60**, 781 (1988).
- [15] X. I. Qi, and S.C. Zhang, Rev. Mod. Phys. **83**, 1057 (2011).
- [16] X.G. Wen, Quantum field theory of many-body systems (Oxford University Press, 2004).
- [17] X.L.Qi, T. L. Hughes, and S.C. Zhang, Phys. Rev. B **78**, 195 424 (2008).
- [18] Y. H. Jeong, S.C. Kim, and S.-R. Eric Yang, Phys. Rev. B **91**, 205441 (2015).
- [19] R. D. King-Smith and David Vanderbilt, Phys. Rev. B **47**, 1651 (1993).
- [20] R. Resta, Rev. Mod. Phys. **66**, 899 (1994).
- [21] J. Zak, Phys. Rev. Lett. **62**, 2747 (1989).
- [22] P. Delplace, D. Ullmo, G. Montambaux, Phys. Rev. B, 195452 **84**, (2011).
- [23] Y. Hatsugai, J. Phys. Soc. Jpn., **75**, 123601 (2006).
- [24] S.C. Kim, P.S. Park, and S.-R. Eric Yang, Phys. Rev. B **81**, 085432 (2010).
- [25] C. Tang, W. Yan, Y. Zheng, G. Li, and L. Li, Nanotechnology **19**, 435401 (2008).
- [26] M. F. Atiyah and I. M. Singer, Ann. Math. **87**, 484(1968), M. F. Atiyah and I. M. Singer, Ann. Math. **93**, 119(1971).
- [27] J.C. Y. Teo, L.Fu, and C.L. Kane, Phys. Rev B **78**, 045426 (2008).
- [28] S. Ryu and Y. Hatsugai, Phys. Rev. Lett. **89**, 077002 (2002).
- [29] J. Pachos and M. Stone, Int. J. Mod. Phys. B **21**, 5113 (2007).
- [30] M. Igami, T. Nakanishi, and T. Ando, J.Phys. Soc. Jpn., **68**, 716 (1999); S.-R. Eric Yang and H.C. Lee, Phys. Rev. B **76**, 245411 (2007).
- [31] J. K. Pachos, Comtemporary Physics **50**, 375 (2009).
- [32] K. Wakabayashi, K.-I. Sasaki, T. Nakanishi, and T. Enoki, Sci. Technol. Adv. Mater. **11** 054504 (2010).
- [33] S.C. Kim and S.-R. Eric Yang, J. Phys.:Condens Matter, **24**, 195301 (2012).
- [34] S.C. Kim and S.-R. Eric Yang, Annals Phys.(NY) **347**, 21 (2014).
- [35] Note that  $\text{Arg}[\prod_i z_i] \neq \sum_i \text{Arg}[z_i]$  since  $\sum_i \text{Arg}[z_i]$  can be much larger than  $2\pi$ .